Appendix: Effect of non-hydrostatic stress

The velocities and refractive indices presented in the main text were measured in samples compressed quasi-hydrostatically during seven pressure cycles, yielding ±2% scatter in V_P, V_S, and n. Data were omitted from the main text from the three pressure cycles in which the sample was pressed against both diamonds without a significant layer of soft medium to distribute stress. Figs. S1-S2 show these data.

Two of the previously omitted pressure cycles were from the wollastonite powder sample that was purposefully loaded without a pressure medium. One was the second pressure cycle of a sample loaded with an argon medium. In this case, when the laser was focused on the glass sample, there was no Brillouin peak from argon (i.e. no peak at ~8 GHz in the cyan spectrum in Fig. S2), meaning that a negligibly thin layer of argon separates the sample from the diamond anvils. Instead, the majority of the argon must have been squeezed away from the sample region during the two pressure cycles. During these three compression runs without a substantial pressure medium, Fig. S1 shows that non-hydrostatic stress (and resulting strain) causes a 4% systematic reduction of sound speed between 20 and 40 GPa.

We hypothesize that changes in atomic packing (coordination changes) during non-hydrostatic compression cause the observed sound-speed reduction; shear stresses activate rearrangements of atoms into denser packings, which cause decreases in V_P and V_S (Fig. S1). This hypothesis is also consistent with most of the decompression data: sound speeds during decompression following non-hydrostatic compression are slightly lower than other decompression data between 40 and 20 GPa (empty cyan squares in Fig. S1). Nonetheless, as in the case of quasi-hydrostatic compression, sound speeds return to their original values upon decompression to 0 GPa.

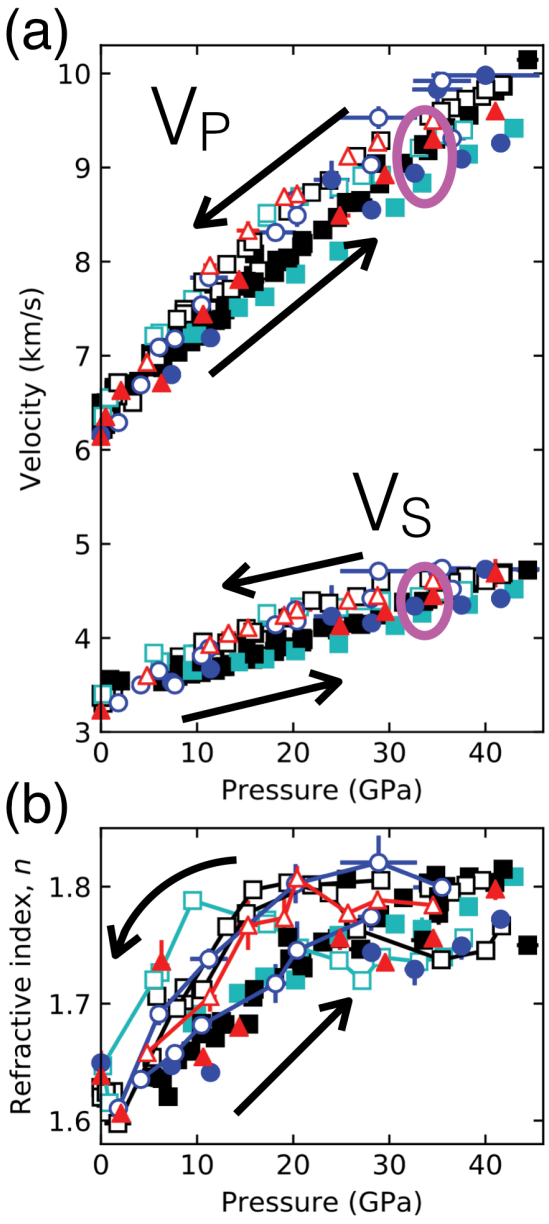

FIGURE S1. All sound speeds (**a**) and refractive indices (**b**) measured in the present study upon compression (solid symbols) and decompression (open symbols), as a function of pressure, including non-hydrostatically compressed samples. Black squares and red triangles represent, respectively, melt-quenched and pressure-amorphized material that is quasi-hydrostatically compressed. The powder compressed with no pressure medium is shown as blue circles, while a pressure run in which a melt-quenched glass bridged the two diamond anvils is shown in cyan squares. Sound speeds derived from the raw data of Figure S2 are circled in pink. Line segments connect data points during individual decompression runs in panel **b**.

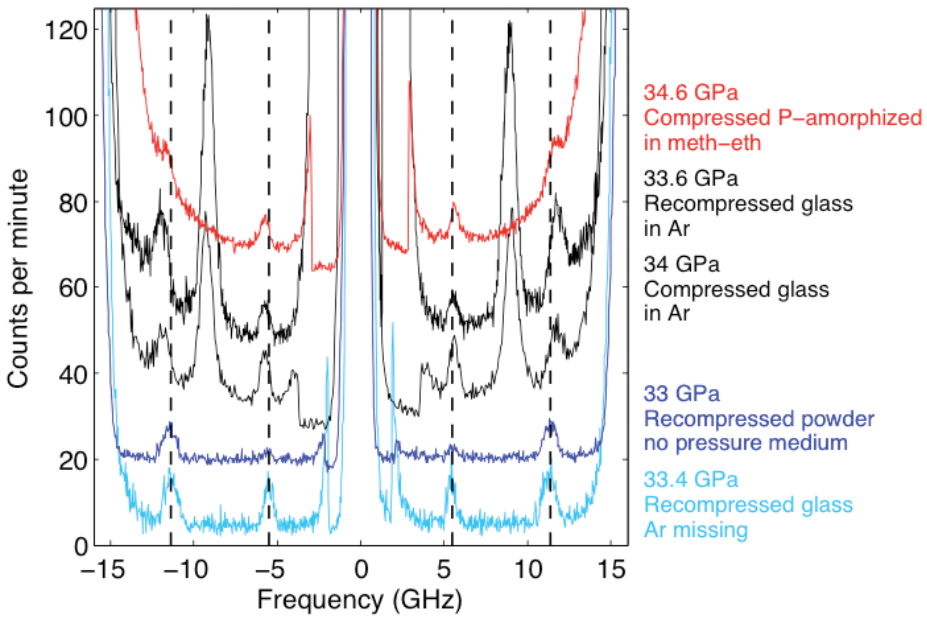

FIGURE S2. Brillouin spectra at 34 (±1) GPa obtained in five different compression runs that are described to the right of the figure. Photon counts are normalized to one-minute collection time, vertically offset, and plotted vs. the frequency shift of the photon. Black dashed lines mark the positions of Brillouin peaks in non-hydrostatically compressed samples (both the powdered wollastonite compressed with no pressure medium, and the glass starting material that is separated from the gasket by argon but not from the diamond anvils). Black peaks at ±8 GHz are from longitudinal phonons in argon, peaks at ±16 GHz are from shear phonons in diamond, and the apparent broadening of diamond peaks in the red spectrum is caused by longitudinal phonons in methanol-ethanol.